*Carbohydrate Polymers* **6** (1986) 321–333

# Concentration Regimes in Xanthan Gum Solutions Deduced from Flow and Viscoelastic Properties

G. Cuvelier and B. Launay

Food Science Department, ENSIA, Massy, France

(Received: 31 January 1986)

## *SUMMARY*

*The rheological properties of aqueous xanthan solutions have been studied in 0·1* M *NaCl at 25 °C at concentrations up to 0·8 g dl*$^{-1}$*. Two critical concentrations are found from viscosity measurements:* $C^* = 0{\cdot}03$ *g dl*$^{-1}$*, the limit of the dilute domain, and* $C^{**} = 0{\cdot}11$ *g dl*$^{-1}$ *beyond which* $\eta_{\mathrm{sp}_0}$ *varies as* $C^{4{\cdot}2}$*. The viscoelastic properties also show evidence of a critical concentration close to* $C^{**}$*. On each side of* $C^{**}$*, a different master curve is obtained using a time–concentration superposition principle. Beyond* $C^{**}$*, the density of junction zones of the elastic network does not seem to increase. A mechanism of parallel packing of chain segments could explain these results. This mechanism is compatible with the rigid structure of the xanthan chain and is in agreement with the hypothesis of side-by-side association proposed by several authors.*

## INTRODUCTION

In recent years, xanthan gum, the extracellular polysaccharide produced by fermentation of the bacterium *Xanthomonas campestris*, has been shown to be of great interest in many industrial applications, particularly enhanced oil recovery, and in the food industry. A review of production, properties and applications of this biopolymer has been recently published by Kennedy & Bradshaw (1984).

*Carbohydrate Polymers* 0144-8617/86/$03.50 — © Elsevier Applied Science Publishers Ltd, England, 1986. Printed in Great Britain

The primary structure of the molecule is now well-known (Jansson *et al.*, 1975); it consists of a pentasaccharide repeating unit formed by a (1-4)-β-D-glucan backbone linked to a charged trisaccharide side-chain (β-D-mannopyrannosyl-(1-4)-α-D-glucopyrannosyl-(1-2)-β-D-mannopyrannosyl-6-O-acetate) at the 3 position on alternate glucose residues. A pyruvic acid is acetal-linked to the terminal mannose residue with a variable degree of substitution.

In aqueous solution, the thermal transition from an ordered helical structure to a disordered structure has been studied by many physical techniques: optical rotatory dispersion (ORD), circular dichroism, nuclear magnetic resonance (NMR) and viscosity. It occurs at higher temperatures with increasing ionic strength, but the nature of the conformation in the ordered state, mono- or multistranded helix, is still debated (Holzwarth & Prestridge, 1977; Holzwarth, 1978; Norton *et al.*, 1980; Paradossi & Brant, 1982; Paoletti *et al.*, 1983; Muller *et al.*, 1984; Sato *et al.*, 1984). Recently, Milas & Rinaudo (1984) proposed the existence of two ordered conformations in solution with different hydrodynamic characteristics, dependent on the thermal history of the sample.

In the ordered state, aqueous solutions of xanthan show very high low-shear-rate viscosities and pronounced shear thinning behavior. Rigid rod or semi-rigid wormlike models have been proposed to interpret these particular hydrodynamic properties (Holzwarth, 1978, 1981; Whitcomb & Macosko, 1978; Rinaudo & Milas, 1978; Chauveteau, 1982; Paradossi & Brant, 1982; Southwick *et al.*, 1982; Morris *et al.*, 1983; Ross-Murphy *et al.*, 1983; Muller *et al.*, 1984). A tendency to intermolecular association forming non-permanent aggregates has been shown (Southwick *et al.*, 1980, 1981, 1982; Jamieson *et al.*, 1983; Tako & Nakamura, 1984), and it has also been proposed that the aggregates can be disrupted reversibly under shear (Frangou *et al.*, 1982; Morris *et al.*, 1983; Ross-Murphy *et al.*, 1983).

The influence of the solvent on intrinsic viscosity and flow properties of xanthan solutions has been interpreted on the basis of this self-association hypothesis (Launay *et al.*, 1984).

The present study aims to describe more completely the flow and viscoelastic properties of xanthan gum solutions from dilute to semi-dilute conditions in 0·1 M NaCl at 25°C, corresponding to the ordered state of the molecules.

## MATERIALS AND METHODS

Xanthan gum was a commercial food grade sample: Rhodigel 23 (Na form, degree of pyruvylation 1/3, acetate 100%), kindly supplied by Rhône-Poulenc, France.

Solutions were prepared by dispersing the required amount of gum (dry basis) in 200 ml of 0·1 M NaCl, by stirring at room temperature for 30 min, then at 80°C for 1 h. Concentrations $< 0{\cdot}08$ g dl$^{-1}$ were obtained by diluting 0·1 or 0·2 g dl$^{-1}$ solutions with 0·1 M NaCl. All measurements were performed at 25°C.

Flow curves were obtained with two coaxial cylinder viscometers: the Contraves Low Shear 30 ($R_1/R_2 = 0{\cdot}92$, $\dot{\gamma}$ from 0·017 to 128 s$^{-1}$) and the Contraves Rheomat 30 fitted with the double shearing system MSO ($R_1/R_2 = R_3/R_4 = 0{\cdot}98$, $\dot{\gamma}$ from 0·23 to 1720 s$^{-1}$). The results from the two viscometers overlapped satisfactorily (Fig. 1).

Flow curves were fitted using a computerized non-linear regression analysis based on the Newton–Raphson method.

Dynamic measurements were performed using a Rheometrics Fluids Rheometer fitted with a coaxial cylinder system ($R_1/R_2 = 0{\cdot}96$). The frequency range was from $10^{-2}$ to $10^{2}$ rad s$^{-1}$ and three strain

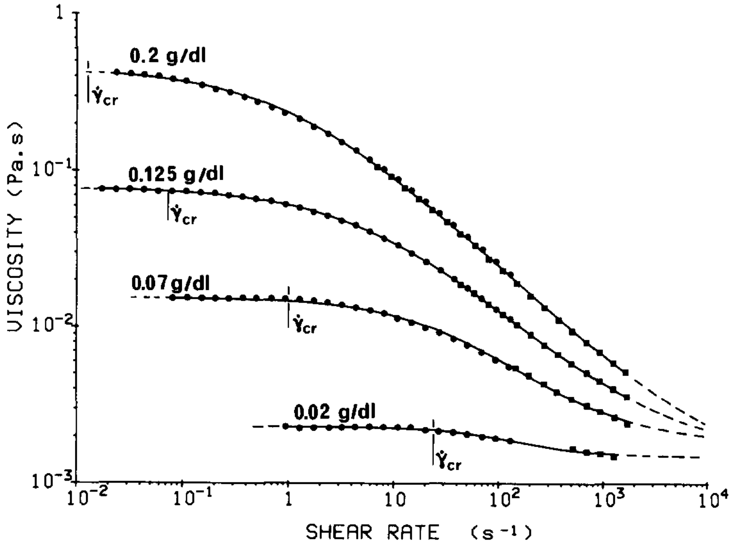

Fig. 1. Flow curves of xanthan solutions. Experimental data: ●, Low shear 30; ■, Rheomat 30; ——, fitted curve (eqn (1)). At $\dot{\gamma} = \dot{\gamma}_{cr}$, $\eta = 0{\cdot}95\eta_0$.

amplitudes (10, 20 and 30%) were used to check that the measurements were performed in the linear domain. The results reported relate to linear viscoelastic behavior when $G'(\omega)$ and $G''(\omega)$ are independent of the strain amplitude.

## RESULTS AND DISCUSSION

Flow curves have been obtained over the wide concentration range ($5 \times 10^{-3} - 5 \times 10^{-1}$ g dl$^{-1}$), and examples of these are given in Fig. 1. The limiting zero shear rate Newtonian viscosity $\eta_0$ is experimentally attainable for concentrations up to $C = 0{\cdot}2$ g dl$^{-1}$. When the concentration decreases, the beginning of the shear thinning zone ($\dot{\gamma} = \dot{\gamma}_{\mathrm{cr}}$) is shifted towards higher shear rates. It can be seen from Fig. 1 that shear thinning behavior is still discernable in dilute solutions ($C < C^*$). At high shear rates, the second Newtonian zone, $\eta_\infty$, is approached.

From $\eta_0$ values at very low concentrations (up to 0·015 g dl$^{-1}$), we have determined an intrinsic viscosity $[\eta]_0$ of 49·3 dl g$^{-1}$. This value is in agreement with those obtained on other xanthan samples produced by Rhône-Poulenc, France (purified and microgel free) (Chauveteau, 1982) and Kelco, USA (Jamieson *et al.*, 1983).

In order to describe the whole flow curve and study the effect of polymer concentration, we have fitted the following equation to the experimental data:

$$\eta = \eta_\infty + \frac{\eta_0 - \eta_\infty}{1 + (\tau\dot{\gamma})^m} \tag{1}$$

where $\eta_0$ and $\eta_\infty$ are the low and high shear rates' Newtonian viscosities, respectively, $\tau$ is a relaxation time and $m$ a dimensionless exponent. This equation was first derived by Cross (1965) for suspensions, and Soong & Shen (1981) have proposed a similar equation based on a kinetic network model for polymer solutions and melts. This model has been previously used for random coil polysaccharides (galactomannans) by Doublier & Launay (1976, 1981) and Fig. 1 shows that it also describes xanthan flow curves very well. It allows extrapolated values of $\eta_0$ to be obtained when this Newtonian zone has not been reached experimentally ($C > 0{\cdot}2$ g dl$^{-1}$).

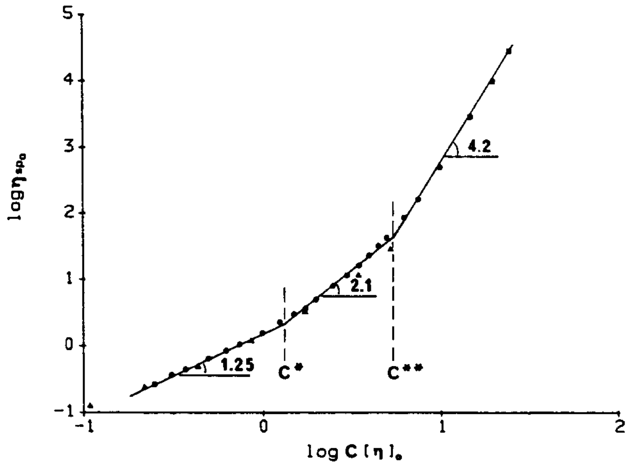

**Fig. 2.** Determination of critical concentrations $C^*$ and $C^{**}$: ●, Experimental $\eta_0$ values; ■, extrapolated values (eqn (1)); ▲, values calculated from Chauveteau (1982).

Figure 2 shows the variation in the zero shear Newtonian specific viscosity with the reduced concentration $C[\eta]_0$; such a master curve representation is classically used for polymer solutions to take into account differences between hydrodynamic dimensions of different samples and to determine the transition from the dilute to semi-dilute regimes. It has been applied to galactomannan solutions (Doublier & Launay, 1976, 1981; Robinson *et al.*, 1982) and other random coil polysaccharide solutions (Morris *et al.*, 1981). On this figure we have added the data calculated from the results of Chauveteau (1982) obtained on a microgel-free sample ($[\eta]_0 = 43$ g dl$^{-1}$). A good superposition is observed, particularly in the dilute zone. Figure 2 reveals two critical concentrations instead of, as is frequently assumed, only one. An analogous result has been reported for synthetic polymer solutions (Kulicke & Klare, 1980), and has also recently been demonstrated for hydroxyethylcellulose solutions in 0·1 M NaCl, this polymer having the same backbone as xanthan (Castelain, 1985). It confirms the results previously observed on another sample of Rhodigel 23 (Launay *et al.*, 1984). Quasi-elastic light scattering data on xanthan solutions at low ionic strengths (Southwick *et al.*, 1981) also showed the presence of two critical concentrations. In this case

$C^* = 0{\cdot}02$ g dl$^{-1}$ and $C^{**} = 0{\cdot}07$ g dl$^{-1}$, which is comparable to our results when $C^* = 0{\cdot}028$ g dl$^{-1}$ and $C^{**} = 0{\cdot}11$ g dl$^{-1}$. The same authors have also observed a sharp retardation in the diffusional mobility of polystyrene latex spheres in xanthan solutions at $C \approx 0{\cdot}1$ g dl$^{-1}$ (Jamieson *et al.*, 1982).

The large concentration interval between the dilute ($C < C^*$) and semi-dilute ($C > C^{**}$) domains is not observed for random coil polysaccharides, and could be explained by the stiff conformation of xanthan. In the dilute zone ($C < C^*$), the hydrodynamic units do not overlap and $\eta_{\mathrm{sp}_0}$ varies as $C^{1{\cdot}2}$, which is a classical result. The chains begin to overlap at a very low concentration of $C^* = 0{\cdot}028$ g dl$^{-1}$ ($C^*[\eta]_0 = 1{\cdot}4$), and beyond $C^{**} = 0{\cdot}11$ g dl$^{-1}$ ($C^{**}[\eta]_0 = 5{\cdot}5$) $\eta_{\mathrm{sp}_0}$ varies as $C^{4{\cdot}2}$. Such a dependence of specific viscosity on concentration is higher than observed for polysaccharide solutions showing purely physical entanglements where $\eta_{\mathrm{sp}_0}$ varies as $C^{3{\cdot}3\text{–}3{\cdot}7}$ (Doublier & Launay, 1976, 1981; Morris *et al.*, 1981). For xanthan solutions in different solvents, we have previously observed a dependence higher than $C^4$ (Launay *et al.*, 1984) and this has been recently confirmed by Milas *et al.* (1985) who have obtained $\eta_{\mathrm{sp}_0} \propto C^{4{\cdot}24}$ beyond $C[\eta]_0 = 6$. At intermediate concentrations ($C^* < C < C^{**}$), a linear relationship is also observed with an exponent close to 2, a value obtained by Kulicke & Klare (1980) for polyacrylamide in water.

It has been possible to calculate the relaxation time $\tau$ defined by eqn (1) down to $C = 0{\cdot}02$ g dl$^{-1}$. Figure 3 shows a plot of log $\tau$ against log $C$. $\tau$ does not vary much for concentrations up to $0{\cdot}04$ g dl$^{-1}$ which is slightly higher than $C^*$. The Rouse relaxation time (Rouse, 1953) calculated at zero concentration from eqn (2) with $M = 2 \times 10^6$ daltons, and $\eta_s$ = the solvent viscosity is $\tau_R = 2 \times 10^{-3}$ s.

$$\tau_R = \frac{6}{\pi^2}\frac{M}{RT}[\eta]_0\eta_s \qquad (2)$$

This result is lower than our lowest value for the cross relaxation time ($8 \times 10^{-3}$ s), but Rouse theory applies to flexible polymers. For $C^* < C < C^{**}$, $\tau$ varies as $C^{2{\cdot}1}$ and this result is consistent with the theoretical prediction $\tau \propto C^2$ for rigid rods in moderately concentrated solution where rotation is impeded by collisions (Doi, 1975), but the Doi theory predicts at the same time a dependence of viscosity on $C^3$ that is not observed here. Beyond $C^{**}$, the relaxation time

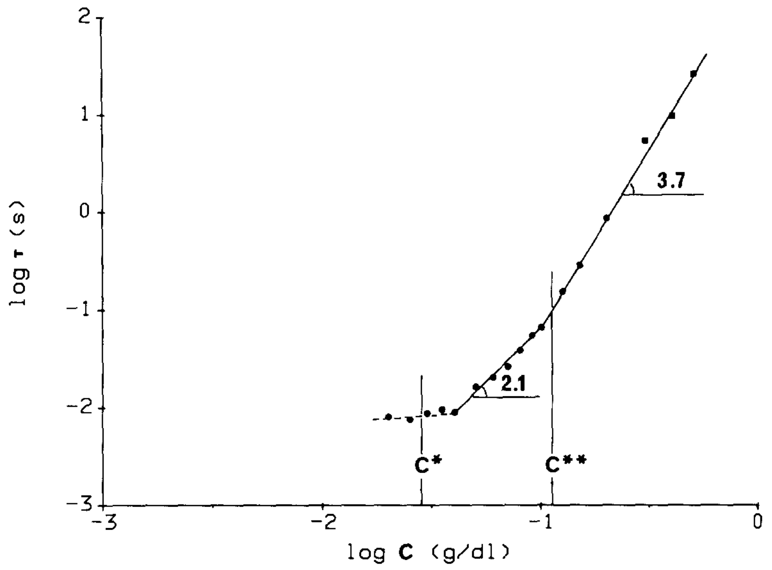

**Fig. 3.** Relaxation time as a function of concentration: ●, ■ — see Fig. 2. The critical concentrations are those determined in Fig. 2.

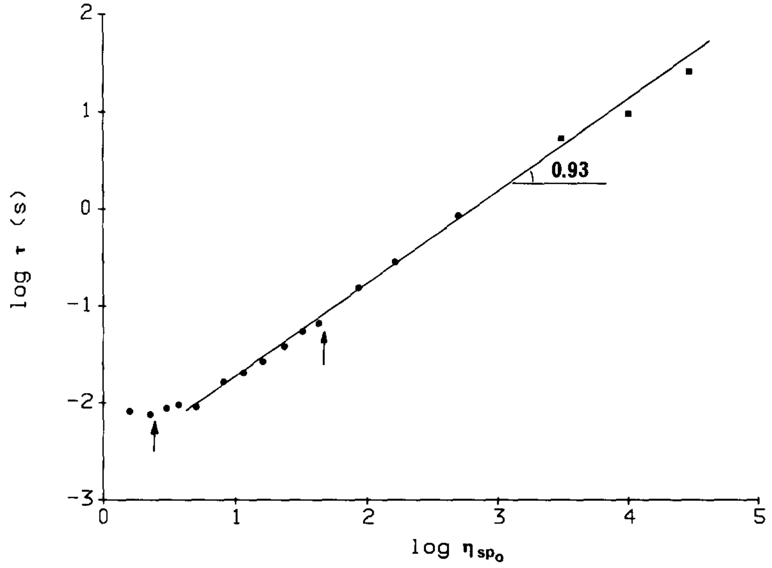

**Fig. 4.** Correlation between relaxation time and reduced specific viscosity in log scales. Arrows correspond to the values of $\eta_{sp_0}$ at $C = C^*$ and $C = C^{**}$: ●, ■ — see Fig. 2.

increases much more with concentration ($C^{3\cdot7}$). Figure 4 shows that the relaxation time remains approximately proportional to $\eta_{\mathrm{sp}_0}$ beyond $C^*$.

## VISCOELASTIC PROPERTIES

Dynamic measurements have been performed from $C = 0\cdot025$ to $0\cdot8$ g dl$^{-1}$. The variation of the loss ($G''$) and storage ($G'$) modulus with $\omega$ (Fig. 5) shows that the viscoelastic behavior changes from a weakly elastic to a rubber-like liquid when the concentration increases. At high concentrations, these results are comparable to those obtained by Frangou *et al.* (1982) at $C = 0\cdot5$ g dl$^{-1}$, and consistent with those reported by Lim *et al.* (1984) at 1 g dl$^{-1}$.

Figure 6 shows the variation with concentration of the frequency corresponding to the beginning of the elastic plateau zone ($\omega_p$) when $G'$ becomes greater than $G''$. It is noteworthy that different behavior is observed on each side of $C^{**}$. Above $C = C^{**}$, the beginning of the elastic plateau is shifted towards lower frequencies, as expected; however, in the intermediate concentration domain ($C^* < C < C^{**}$), the

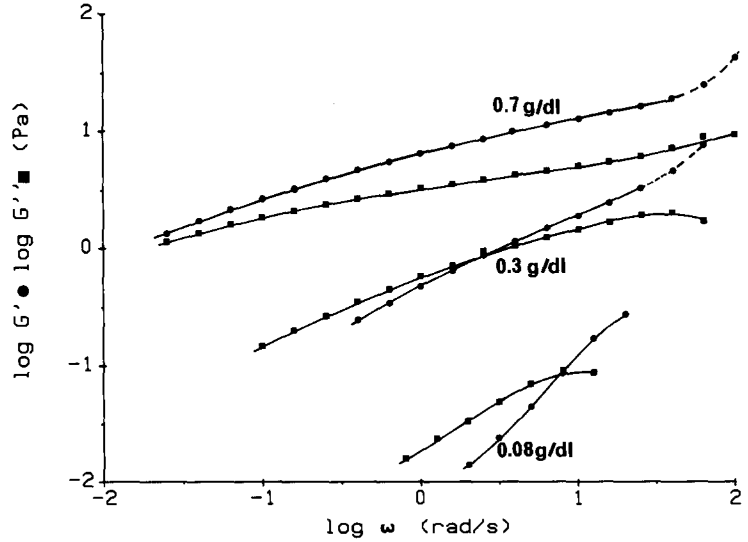

**Fig. 5.** The loss ($G''$), ■, and storage ($G'$), ●, modulus as a function of frequency—effect of concentration. The dashed part of the line corresponds to experimental results which are not superimposed on the master curve (see Fig. 8).

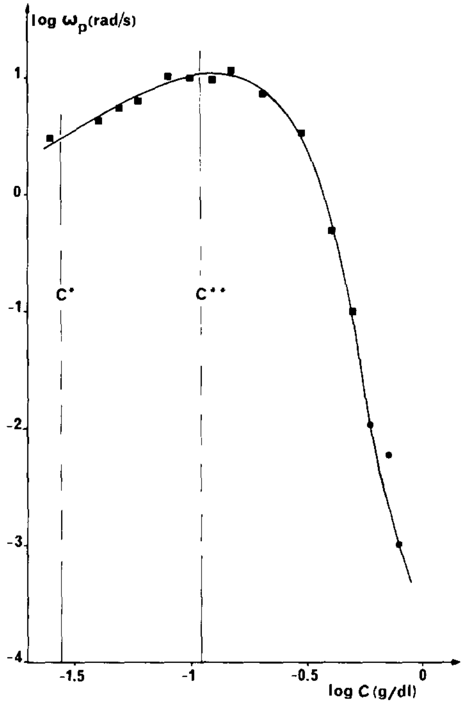

**Fig. 6.** Concentration dependence of the beginning of the elastic plateau zone ($G' = G''$ at $\omega = \omega_p$); the last three points are extrapolated from Fig. 8. Critical concentrations from Fig. 2.

shift is much smaller and in the reverse direction. Therefore, two time–concentration superposition strategies have to be applied, depending on the concentration range. Master curves are shown for $C \leqslant 0{\cdot}125$ g dl$^{-1}$ (Fig. 7) and for $C > 0{\cdot}125$ g dl$^{-1}$ (Fig. 8). A few results obtained at the highest frequencies for $C > C^{**}$ did not superimpose on the master curve; no satisfactory explanation has been found for this.

In Fig. 9, the corresponding modulus and frequency shift factors $a_g$ and $a_f$, respectively, are plotted against concentration on a logarithmic scale. The modulus shift factor $a_g$ varies as $C^{-2{\cdot}9}$ for $C^* < C < C^{**}$, and stays equal to 1 for $C > C^{**}$. Therefore it may be assumed that the network density levels off beyond $C^{**}$. This phenomenon could be explained by the high extension of xanthan which would bring about parallel packing of chain segments. Adding a new chain could only

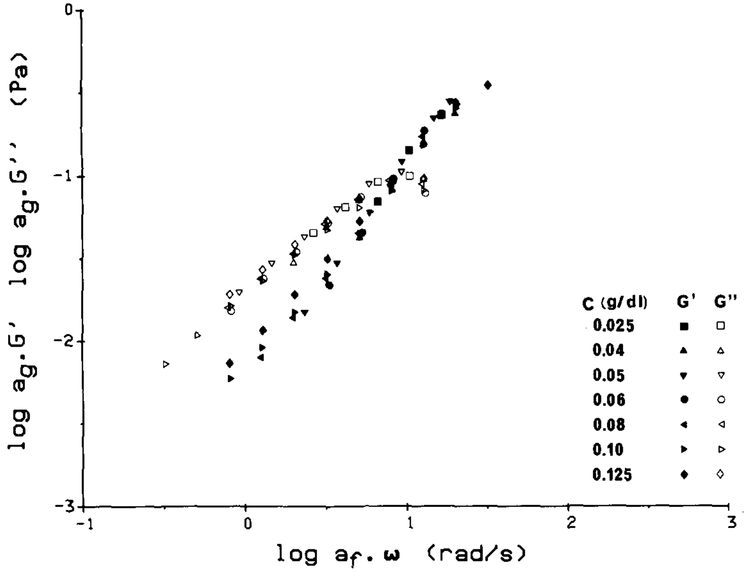

**Fig. 7.** Time-concentration superposition applied for $C \leqslant 0{\cdot}125$ g dl$^{-1}$. Reference concentration 0·08 g dl$^{-1}$.

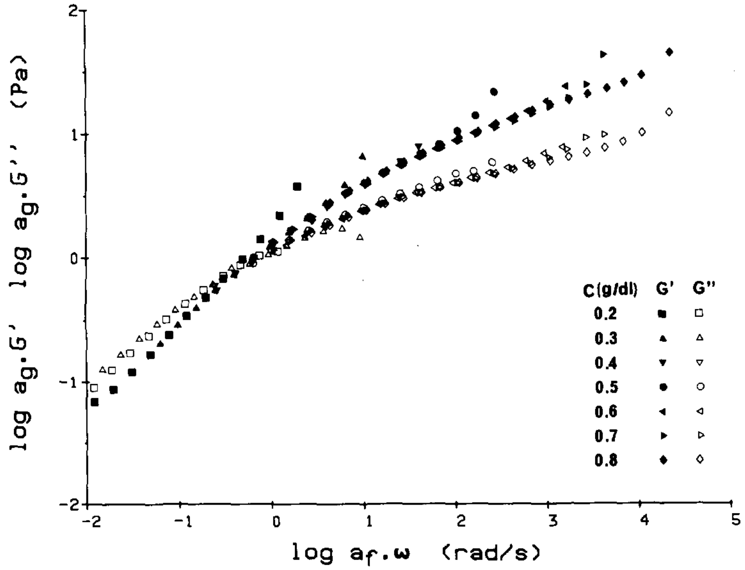

**Fig. 8.** Time-concentration superposition applied for $C > 0{\cdot}125$ g dl$^{-1}$. Reference concentration 0·4 g dl$^{-1}$.

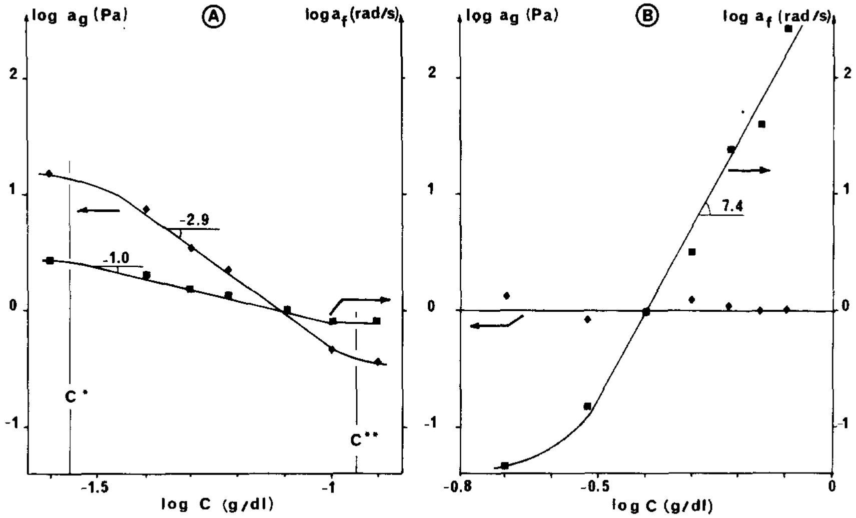

**Fig. 9.** Concentration dependence of modulus ($a_g$) and frequency ($a_f$) shift factors: A, $C \leqslant 0{\cdot}125$ g dl$^{-1}$; B, $C > 0{\cdot}125$ g dl$^{-1}$. Critical concentrations from Fig. 2.

reinforce existing junction zones without creating any new ones. However, such a mechanism would bring about a large increase in the lifetime of these junction zones and, therefore, could explain the very high dependence of the time shift factor $a_f$ on concentration beyond $C^{**}$ ($a_f \propto C^{7{\cdot}4}$).

## CONCLUSION

From complementary and consistent rheological measurements of both flow and viscoelastic properties, the role of concentration in xanthan solution is described and it is possible to get some insight into the structure of the solution.

The dilute domain exists only up to very low concentrations ($C < C^* = 0{\cdot}03$ g dl$^{-1}$). Overlapping takes place from this concentration, and for $C^* < C < C^{**}$ weak elastic behavior is observed when $\eta_{\text{sp}_0}$ varies approximately as $C^2$. Beyond $C^{**}$, the solution exhibits stronger elastic behavior, with much less frequency dependence and a pseudo-elastic plateau zone at high frequencies. A transitory chain–chain network certainly exists, but, since no increase in the density of the elastic network is observed beyond this second critical concentration, it is clear that the structure of the solution cannot be described by a classical polymer entanglement mechanism. A process based on parallel packing of xanthan chain segments seems more appropriate to explain these properties. The propensity of xanthan to self-association demonstrated by other methods, especially quasi-elastic light scattering (Southwick *et al.*, 1980; Frangou *et al.*, 1982; Jamieson *et al.*, 1983), and the phenomenon of side-by-side association postulated by Morris *et al.* (1983), and taken as responsible for the 'weak gel' properties of xanthan solutions (Ross-Murphy *et al.*, 1983), is consistent with this hypothesis. Domains of associated chains, which are stabilized by hydrogen bonds, are not disrupted by low amplitude oscillatory strains in the linear viscoelastic region but are reversibly disrupted under large shear strains. This could explain the marked shear-thinning behavior of xanthan solutions and also the greater dependence of $\eta_{sp_0}$ on $C$ at concentrations beyond $C^{**}$, compared with entangled 'random coil' polymer solutions. The high values of the relaxation time for $C > C^{**}$ show that the mean lifetime of the junction zones in xanthan solutions may be assumed to be longer than that of junction zones formed by purely physical entanglements. In the same concentration range, the very high dependence on concentration of the complex modulus time shift factor and the relaxation time adds support to the former hypothesis.

## REFERENCES

Castelain, C. (1985). *Thèse de doctorat ENSIA*, Univ. Paris VII et Paris XI, Reg. No. 61.

Chauveteau, G. (1982). *J. Rheology* **26**, 111.

Cross, M. M. (1965). *J. Colloid Sci.* **20**, 417.

Doi, M. (1975). *J. Phys. (Paris)* **36**, 607.

Doublier, J. L. & Launay, B. (1976). *Proceed. 6th Int. Cong. Rheology*, Gothenburg, p. 532.

Doublier, J. L. & Launay, B. (1981). *J. Texture Studies* **12**, 151.

Frangou, S. A., Morris, E. R., Rees, D. A., Richardson, R. K. & Ross-Murphy, S. B. (1982). *J. Polym. Sci., Polym. Letters Ed.* **20**, 531.

Holzwarth, G. (1978). *Carbohydr. Res.* **66**, 173.

Holzwarth, G. (1981). *Am. Chem. Soc. Symp. Ser.* **150**, 15.

Holzwarth, G. & Prestridge, E. B. (1977). *Science* **197**, 757.

Jamieson, A. M., Southwick, J. G. & Blackwell, J. (1982). *J. Polym. Sci., Polym. Phys. Ed.* **20**, 1513.

Jamieson, A. M., Southwick, J. G. & Blackwell, J. (1983). *Faraday Symp. Chem. Soc.* **18**, 131.

Jansson, P. E., Kenne, L. & Lindberg, B. (1975). *Carbohydr. Res.* **45**, 275.

Kennedy, J. F. & Bradshaw, I. J. (1984). *Prog. Ind. Microbiol.* **19**, 319.

Kulicke, W. M. & Klare, J. (1980). *Angew. Makromol. Chem.* **84**, 67.

Launay, B., Cuvelier, G. & Martinez-Reyes, S. (1984). In *Gums and stabilisers for the food industry,* Vol. 2, eds G. O. Phillips, D. J. Wedlock and P. A. Williams, London, Pergamon Press, p. 79.

Lim, T., Uhl, J. T. & Prud'homme, R. K. (1984). *J. Rheology* **28**, 367.

Milas, M. & Rinaudo, M. (1984). *Polym. Bulletin* **12**, 507.

Milas, M., Rinaudo, M. & Tinland, B. (1985). *Polym. Bulletin* **14**, 157.

Morris, E. R., Cutler, A. N., Ross-Murphy, S. B. & Rees, D. A. (1981). *Carbohydr. Polym.* **1**, 5.

Morris, V. J., Franklin, D. & L'Anson, K. (1983). *Carbohydr. Res.* **121**, 13.

Muller, G., Lecourtier, J., Chauveteau, G. & Allain, C. (1984). *Makromol. Chem., Rapid Commun.* **5**, 203.

Norton, I. T., Goodall, D. M., Morris, E. R. & Rees, D. A. (1980). *J. Chem. Soc., Chem. Commun.* 545.

Paoletti, S., Cesaro, A. & Delben, F. (1983). *Carbohydr. Res.* **123**, 173.

Paradossi, G. & Brant, D. A. (1982). *Macromolecules* **15**, 874.

Rinaudo, M. & Milas, M. (1978). *Biopolymers* **17**, 2663.

Robinson, G., Ross-Murphy, S. B. & Morris, E. R. (1982). *Carbohydr. Res.* **107**, 17.

Ross-Murphy, S. B., Morris, V. J. & Morris, E. R. (1983). *Faraday Symp. Chem. Soc.* **18**, 115.

Rouse, P. E. (1953). *J. Chem. Phys.* **21**, 1272.

Sato, T., Norisuye, T. & Fujita, H. (1984). *Polym. J.* **16**(4), 341.

Soong, D. & Shen, M. (1981). *J. Rheology* **25**(2), 259.

Southwick, J. G., Lee, H., Jamieson, A. M. & Blackwell, J. (1980). *Carbohydr. Res.* **84**, 287.

Southwick, J. G., Jamieson, A. M. & Blackwell, J. (1981). *Macromolecules* **14**, 1728.

Southwick, J. G., Jamieson, A. M. & Blackwell, J. (1982). *Carbohydr. Res.* **99**, 117.

Tako, M. & Nakamura, S. (1984). *J. Agric. Biol. Chem.* **48**(12), 2987.

Whitcomb, P. J. & Macosko, W. (1978). *J. Rheology* **22**(5), 493.